

An Ultramicroporous Metal–Organic Framework for High Sieving Separation of Propylene from Propane

Bin Liang,[§] Xin Zhang,[§] Yi Xie, Rui-Biao Lin,^{*} Rajamani Krishna, Hui Cui, Zhiqiang Li, Yanshu Shi, Hui Wu, Wei Zhou,^{*} and Banglin Chen^{*}



Cite This: *J. Am. Chem. Soc.* 2020, 142, 17795–17801



Read Online

ACCESS |



Metrics & More

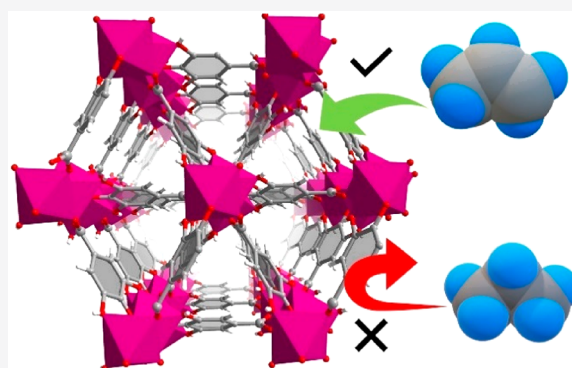


Article Recommendations



Supporting Information

ABSTRACT: Highly selective adsorptive separation of olefin/paraffin through porous materials can produce high purity olefins in a much more energy-efficient way than the traditional cryogenic distillation. Here we report an ultramicroporous cobalt gallate metal–organic framework (Co-gallate) for the highly selective sieving separation of propylene/propane at ambient conditions. This material possesses optimal pore structure for the exact confinement of propylene molecules while excluding the slightly large propane molecules, as clearly demonstrated in the neutron diffraction crystal structure of Co-gallate Co_3D_6 . Its high separation performance has been confirmed by the gas sorption isotherms and column breakthrough experiments to produce the high purity of propylene (97.7%) with a high dynamic separation productivity of $36.4 \text{ cm}^3 \text{ cm}^{-3}$ under ambient conditions. The gas adsorption measurement, pore size distribution, and crystallographic and modeling studies comprehensively support the high sieving $\text{C}_3\text{H}_6/\text{C}_3\text{H}_8$ separation in this MOF material. It is stable under different environments, providing its potential for the industrial propylene purification.



It is stable under different environments, providing its potential for the industrial propylene purification.

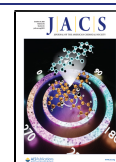
INTRODUCTION

Propylene is a prime olefin feedstock in the petrochemical industry for the manufacture of a variety of chemical commodities, including polypropylene. Due to the good resistance to fatigue, heat, and organic solvents, polypropylene has been widely used for films, fibers, containers, packaging, and especially for personal protective medical or laboratory items.¹ The worldwide production capacity of propylene was up to 114 million metric tons in 2015. It is essential to upgrade the propylene/propane mixture to high-purity propylene in order to produce polypropylene.^{2,3} Compared to ethylene and ethane, propylene and propane show a higher similarity in their physical properties such as volatilities. Specifically, the boiling point difference of propylene/propane is about 5 K, much smaller than that of ethylene/ethane (15 K). The established method for propylene/propane separation involves repeated distillation–compression cycling in giant C3 splitter towers of up to 300 feet high with over 200 trays. The energy consumption of this separation process is theoretically estimated about ~ 12.9 GJ per ton propylene which is much higher than that of ethylene/ethane separation (~ 7.3 GJ per ton ethylene).^{4,5} Therefore, propylene/propane separation is reported as the most capital and energy-intensive distillation process.^{6,7} There is a great demand to develop alternative and energy-efficient separation technologies, including adsorptive separation using porous materials.

As emerging porous materials, metal–organic frameworks (MOFs) feature great capability in pore engineering,^{8–12} especially precise size-tuning and functionalization of the pore surface, and thus have been explored for gas separation and purification.^{13–20} MOFs have been demonstrated as superior adsorbents for many pivotal hydrocarbon separations.^{21–26} In terms of olefin/paraffin separation, MOFs with strong binding sites such as open metal sites can selectively adsorb olefin over paraffin through a π -complexation mechanism. But the coadsorption of the paraffin counterpart usually exists and prevents the production of high-purity olefin.^{27–30} The second approach is to functionalize MOF pore surfaces for preferential binding of paraffin over olefin, which directly produces pure olefin, as demonstrated in ethane/ethylene separation by a few unique MOFs.^{21,31–35} The third approach is to finely tune the pore sizes of MOFs, enabling size exclusion of the large molecule for high sieving separation, as exemplified by few examples.^{36–39} Compared with the molecular structure difference between ethylene (C_2H_4) and ethane (C_2H_6), the

Received: September 2, 2020

Published: September 29, 2020



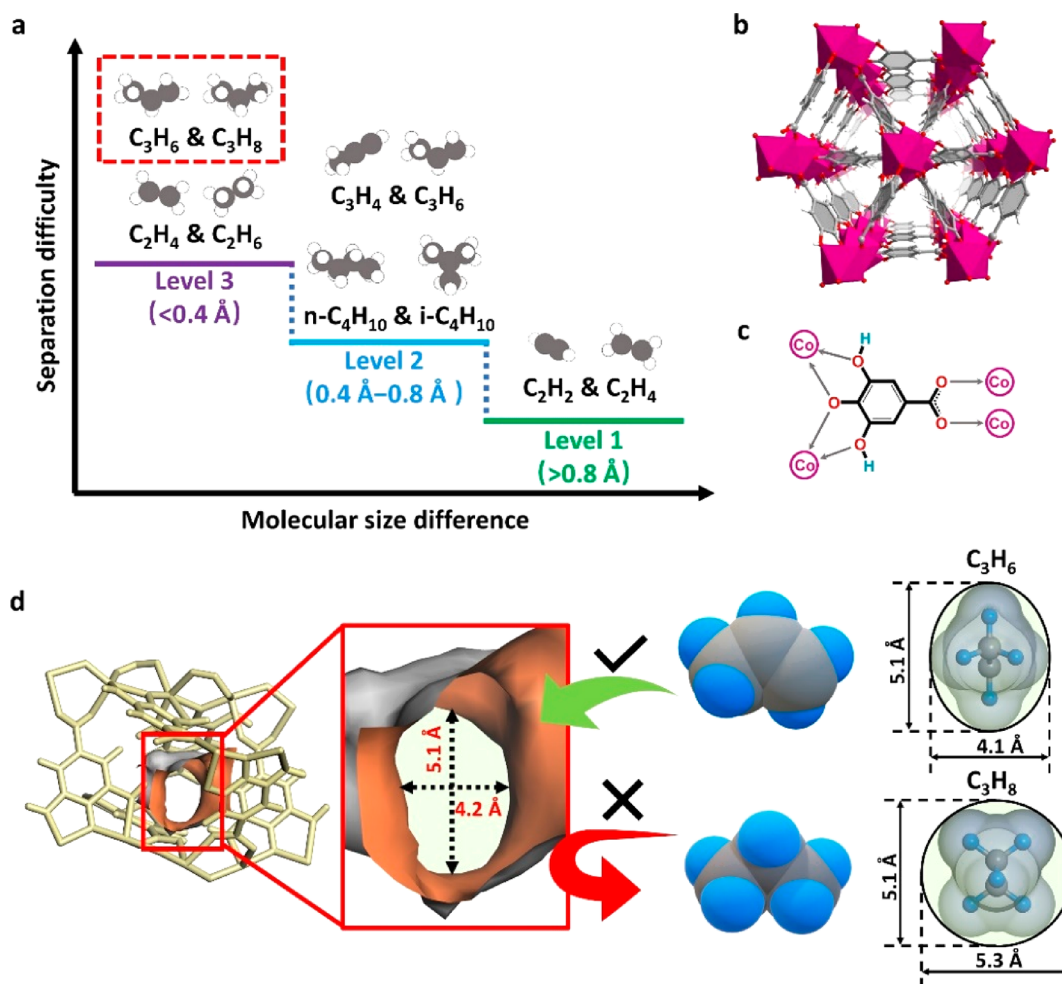


Figure 1. Structure of Co-gallate MOF and rationale for C_3H_6/C_3H_8 separation. (a) The complexity of different hydrocarbon separation systems classified by the molecular size difference. (b) The crystal structure of Co-gallate MOF without guest; purple, red, gray, and white nodes represent Co, O, C, and H atoms, respectively. (c) The coordination mode of the gallate linker. (d) Schematic diagram of the size sieving separation for C_3H_6 and C_3H_8 molecules. Co-gallate MOF shows elliptical pore window with dimensions of 5.1 and 4.2 Å, respectively, which are slightly larger than those of C_3H_6 molecule (5.1 and 4.1 Å, respectively) and smaller than those of C_3H_8 molecule (5.3 and 5.1 Å, respectively).

difference between propylene (C_3H_6) and propane (C_3H_8) molecules is smaller because both molecules have the same alkyl part (i.e., CH_3 group). This smaller difference of molecular structure and size makes either propane-selective separation or propylene sieving separation a more challenging task.^{28,29,40,41} In terms of high sieving separation, compared with other separations of alkyne/alkene and branched/linear alkanes, the subtle molecular size difference of olefin and paraffin (below 0.04 nm, i.e. <math><0.4 \text{ \AA}</math>) makes their separation difficulty at a high level, particularly for C_3H_6/C_3H_8 separation (Figure 1a).

Constructed from a common substance in pharmaceutical industry, gallic acid, a readily available and ultramicroporous MOF Co-gallate was previously reported as high sieving adsorbent for C_2H_4/C_2H_6 separation, that were basically discovered unexpectedly. Here we have carefully analyzed the pore space of this MOF with a discovery of its pore size distribution at 5.2 Å that is between the molecular sizes of propylene and propane, which motivated us to examine its potential for size exclusion of propane from propylene under ambient conditions. The optimal channel size and pore confinement for propylene molecules indeed endows Co-gallate with high sieving separation for propylene from propane

with exceptional selectivity. Furthermore, Co-gallate exhibits both high propylene capacity ($66.6 \text{ cm}^3 \text{ cm}^{-3}$, STP) and dynamic separation productivity ($36.4 \text{ cm}^3 \text{ cm}^{-3}$, STP) according to breakthrough experiments under ambient conditions. The Co-gallate MOF exhibits a clear separation mechanism as validated by pore size analyses and crystallographic and modeling studies. Moreover, the facile synthesis and high water stability of this low-cost MOF also highlight its promise for industrial C_3H_6/C_3H_8 separation in the future.

RESULTS AND DISCUSSION

Co-gallate- $2H_2O$ ($[Co(C_7O_5H_4)] \cdot 2H_2O$) was synthesized under hydrothermal reaction of gallic acid and cobalt chloride in aqueous solution. Because gallic acid has good water solubility, water is used here as reaction medium without the use of any harmful organic solvents. Crystallographic studies based on neutron powder diffraction reveals that the activated Co-gallate crystallizes in the $P3_1$ space group, in which each Co^{2+} ion is octahedrally coordinated by two oxygen atoms from two different carboxylate groups, four oxygen atoms from hydroxyl groups, and two deprotonated μ_2 -O atoms in two gallate ligands (Figure 1b,c). The CoO_6 octahedra are bridged by the linkers to form rod-like infinite cobalt-oxo chains, which

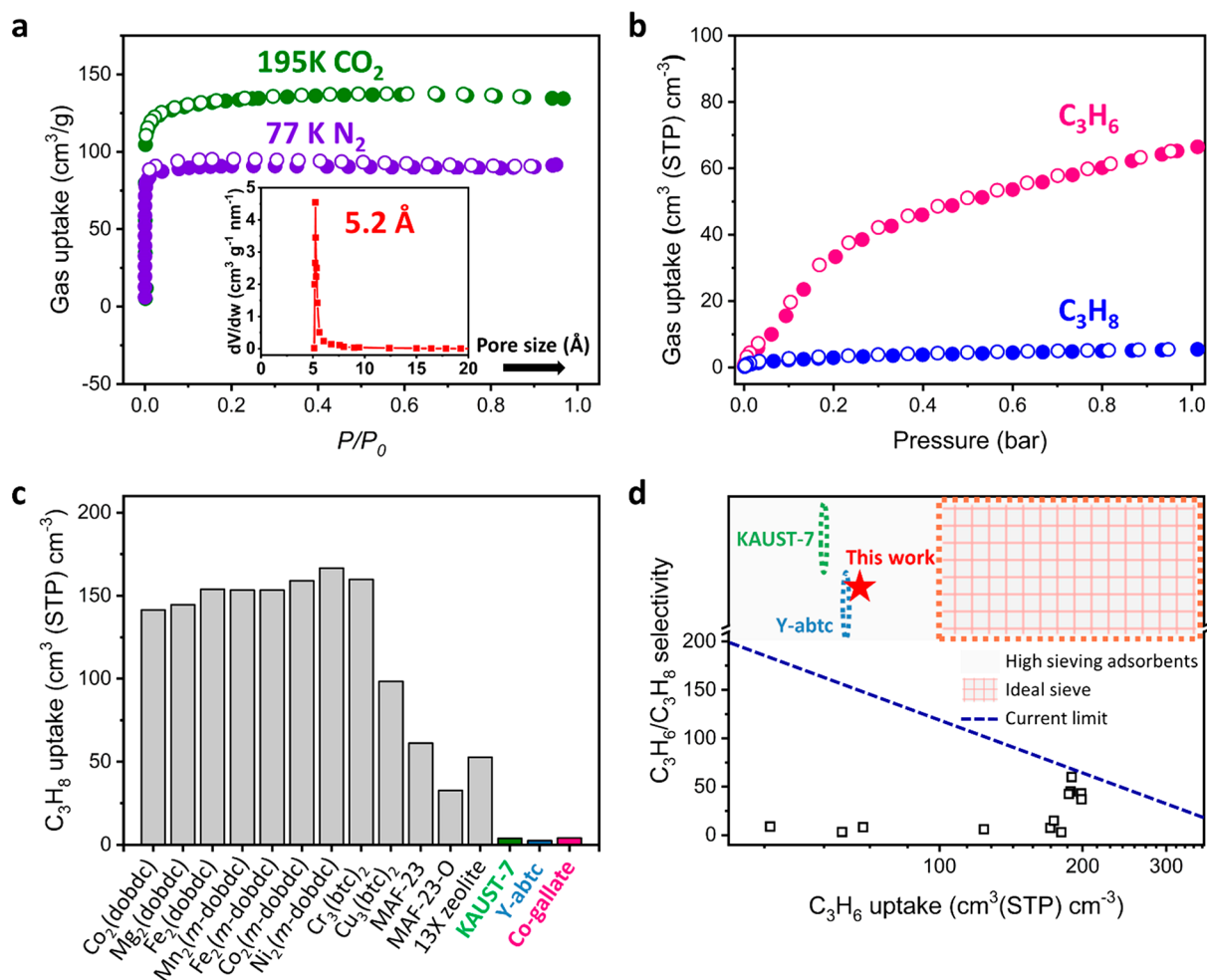


Figure 2. Gas sorption properties of Co-gallate. (a) Single-component sorption isotherms of carbon dioxide at 195 K, nitrogen at 77 K. The inset shows the pore size distribution of Co-gallate MOF (about 5.2 Å) calculated from 77 K N₂ adsorption isotherm based on the Horvath–Kawazoe model. (b) Gas sorption isotherms of propylene and propane at 298 K for Co-gallate. (c) Comparison of propane uptake with reported porous materials.^{28,30,37,38,42} (d) Qualitative comparison of adsorption IAST selectivity with uptake of different porous materials for an equimolar propylene/propane mixture.^{28,30,37,38,42} IAST selectivity of the MOF sieves is largely uncertain associated with the low uptake of propane. Ideal molecular sieves here are defined as those which can completely block C₃H₈ molecules and take up large amount of C₃H₆ molecules from gas mixtures.

are further interconnected into three-dimensional structure. Co-gallate features a three-dimensional branched channel system interconnected by the narrow window between neighboring ligands along the *c* axis. Notably, the narrow elliptical window shows an aperture size of 16.8 Å², which is slightly larger than the minimum cross-sectional area of propylene (16.4 Å²) and smaller than that of propane (21.2 Å²) (Figure 1d and Figure S1), indicating a potential shape-sieving effect for propylene from propane in Co-gallate MOF.

Prior to C₃H₆ and C₃H₈ adsorption measurements, the permanent porosity of Co-gallate was examined by CO₂ adsorption at 195 K and N₂ adsorption at 77 K. The CO₂ and N₂ adsorption isotherms of Co-gallate show reversible type-I adsorption profiles. The total CO₂ and N₂ uptake capacities of Co-gallate are 141.1 and 89.6 cm³ g⁻¹, respectively (Figure 2a). The Brunauer–Emmett–Teller (BET) surface area and pore volume are determined as 486.8 m² g⁻¹ and 0.21 cm³ g⁻¹, respectively, based on the CO₂ adsorption isotherm (Figure S2). Pore size distribution analysis from N₂ adsorption isotherm at 77 K confirms the pore size of Co-gallate MOF is about 5.2 Å, and it is slightly smaller than

the molecular size of propane in the elliptical cylinder model, matching well with the size difference between C₃H₆ and C₃H₈.

Motivated by the optimal pore size of Co-gallate MOF, single-component adsorption isotherms at 298 K were collected to evaluate its C₃H₆/C₃H₈ separation performance. A notable amount of propylene was adsorbed by Co-gallate with an uptake capacity of 66.6 cm³ cm⁻³ (STP) at 1 bar, which is higher than that of the benchmark niobium-based KAUST-7³⁷ (56.8 cm³ cm⁻³, STP) and yttrium-based Y-abtc³⁸ (63.5 cm³ cm⁻³, STP), owing to the slightly larger pore volume of Co-gallate (Figure 2b). The C₃H₆ adsorption capacity of Ni-gallate and Mg-gallate MOF at 298 K and 1 bar are 47.7 and 54.1 cm³ cm⁻³ (STP), respectively (Figure S3). The packing density of C₃H₆ in Co-gallate is calculated to be 0.36 g cm⁻³ (~71% of liquid propylene density). In contrast, Co-gallate only adsorbed a negligible amount of C₃H₈ (5.2 cm³/cm³, STP) at 298 K and 1 bar. This low C₃H₈ uptake is very rare among MOFs for C₃H₆/C₃H₈ separation. The C₃H₈ uptake of Co-gallate (5.2 cm³ cm⁻³, STP) is about 2 orders of magnitude lower than those of M₂(dobdc) and M₂(m-dobdc) (120–163

$\text{cm}^3 \text{cm}^{-3}$, STP, Figure 2c and Table S3).^{28,30,40,41} The Co-gallate MOF with high sieving effect is very promising for the recovery of high-purity C_3H_6 through a pressure swing adsorption (PSA) process due to the negligible coadsorption of C_3H_8 . Notably, there is also no significant C_3H_8 uptake by Co-gallate at different temperatures (273–313 K), whereas the C_3H_6 uptake capacity can further increase to $97.5 \text{ cm}^3 \text{cm}^{-3}$ (STP) at 273 K (Figures S4 and S5). Based on adsorption isotherms at 273 and 298 K, the isosteric heat of adsorption (Q_{st}) was calculated to be 41 kJ mol^{-1} using the virial method (Figures S6 and S7). The apparent adsorption enthalpy is quite low compared with those of other MOFs (Table S3), which is desirable for facile regeneration under mild conditions.

We employed the ideal adsorbed solution theory (IAST) to evaluate the separation selectivity of a $\text{C}_3\text{H}_6/\text{C}_3\text{H}_8$ mixture. The IAST selectivity was calculated to be 330 at 1 bar and 298 K (Figure 2d and Figure S8), which is much higher than those of many top-performing MOFs, such as $\text{Co}_2(\text{dobdc})$ (46), $\text{Mn}_2(\text{dobdc})$ (25), $\text{Fe}_2(m\text{-dobdc})$ (60), $\text{Mn}_2(m\text{-dobdc})$ (43) (Table S3),^{30,40,41} and comparable with those of the benchmark KAUST-7³⁷ and Y-abtc,³⁸ implying its potential for highly efficient separation of C_3H_6 from C_3H_8 . It should be noted that the IAST selectivity for molecular sieves is often subject to uncertainties due to the large error from the ultralow C_3H_8 uptake.

To structurally understand the separation performance of Co-gallate, high-resolution neutron powder diffraction (NPD) of C_3D_6 -loaded Co-gallate MOF was measured to determine the supramolecular interactions between the framework and C_3D_6 molecule (Figure S9). Three types of crystallographically independent C_3D_6 molecules are identified at the intersection of the cross-linking channel system, as shown in Figure 3a. The occupancy of C_3D_6 were refined to be 0.48(2), 0.34(2), and

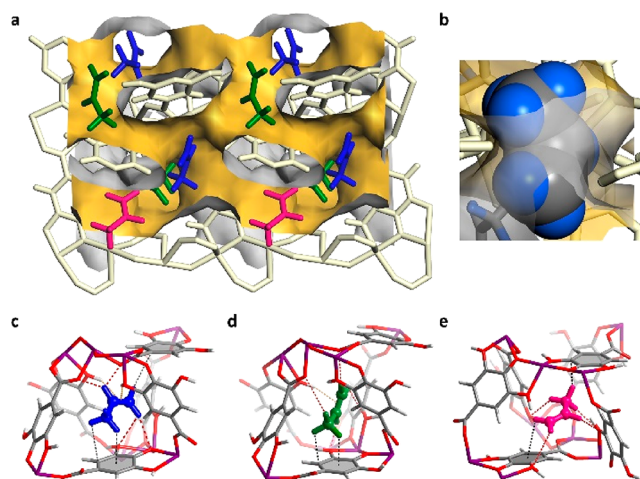


Figure 3. Neutron diffraction crystal structure of Co-gallate-0.38 C_3D_6 and preferential binding sites for C_3D_6 . (a) The packing diagram of the C_3D_6 adsorbed structure. The preferential binding sites for C_3D_6 (site I, site II, and site III) are represented in blue, green, and pink, respectively. The framework and the pore surface are shown in pale gold and yellow. (b) View of the optimal aperture of Co-gallate MOF for exact confinement of propylene molecules. The light blue and gray spheres represent H and C atoms of propylene molecules. (c–e) Three different preferential adsorption sites, site I (c), site II (d), and site III (e), and their close contacts with the framework, with C–D...O, C–D... π , and O–H... π interactions highlighted as red, black, and orange dashed lines, respectively.

0.32(2) at sites I, II, and III, respectively, which corresponds to $62.2 \text{ cm}^3 \text{cm}^{-3}$ (STP), in great agreement with the amount in gas adsorption experiment ($66.6 \text{ cm}^3 \text{cm}^{-3}$, STP) at 1 bar. The C_3D_6 molecules are confined inside the pore through multiple weak interactions among three sites in slightly different binding geometry (Figure 3b, Figures S10 and S11). Specifically, on site III, C–D...O hydrogen bonding ($1.92(4)$ – $3.18(4)$ Å), O–H... π interaction ($2.28(2)$ – $2.87(1)$ Å), and weak van der Waals interactions C–D... π ($2.61(4)$ – $3.15(5)$ Å) are observed between C_3D_6 molecule and the hydroxyl group or the aromatic ring on the ligand (Figure 3c–e and Table S5), enabling the C_3D_6 molecules to accommodate well into the pore structure. In addition, the structural comparison of bare Co-gallate and C_3D_6 -loaded Co-gallate reveals a negligible framework deformation indicating certain rigidity of Co-gallate framework upon guest molecules inclusion (Figure S12). Therefore, the pore structure enables sufficient diffusion and confinement of C_3H_6 into Co-gallate while showing size exclusion for the slightly larger C_3H_8 molecule.

Motivated by the C_3H_8 -exclusion of Co-gallate shown by single component adsorption, we further evaluated its $\text{C}_3\text{H}_6/\text{C}_3\text{H}_8$ separation performance by transient breakthrough simulation, in comparison with several benchmark materials (Figure S13). The simulated breakthrough curve shows that the retention time of C_3H_8 in Co-gallate is negligible as the result of molecular exclusion. In contrast, the retention time of C_3H_8 for $\text{M}_2(m\text{-dobdc})$ and $\text{M}_2(\text{dobdc})$ series are much longer due to their significant coadsorption of C_3H_8 (Figures S14 and S15). Co-gallate also exhibits much higher dynamic selectivity and purity of C_3H_6 in adsorbed phase based on the transient breakthrough curve (Figure S16 and Table S4). Next, we carried out binary gas (50/50 $\text{C}_3\text{H}_6/\text{C}_3\text{H}_8$) column breakthrough measurements (Figure S17). C_3H_8 eluted at the very beginning of the process, indicating no noticeable adsorption of C_3H_8 in the column (Figure 4a) whereas C_3H_6 underwent a long retention time of ~ 28 min. Correspondingly, the dynamic propylene productivity was calculated to be $36.4 \text{ cm}^3 \text{cm}^{-3}$ (STP) (Figure S18), which is higher than that of niobium-based KAUST-7³⁷ ($26.3 \text{ cm}^3 \text{cm}^{-3}$, STP) and comparable to that of yttrium-based Y-abtc³⁸ ($41.1 \text{ cm}^3 \text{cm}^{-3}$, STP). Compared with the equilibrium capacity for C_3H_6 at 0.5 bar, the lower dynamic C_3H_6 adsorption capacity of Co-gallate may be attributed to the relatively slow diffusion of C_3H_6 into the pore channels during the separation process (Figure S19). The adsorbed propylene can be simply desorbed in 14 min by purging pure He gas at room temperature. A small amount of C_3H_8 was detected in the desorbed gas, and the purity of C_3H_6 was calculated to be 97.7% through a single PSA process (Figure 4b and Figure S20). The mild desorption condition can further reduce energy cost as compared to zeolite 4A which requires high desorption temperature.⁴³ To examine the reusability of Co-gallate in multiple cycling separation, five regeneration-breakthrough cycles were performed, and its dynamic productivity was fully retained (Figure 4c, Figures S21 and S22).

Under practical conditions, the $\text{C}_3\text{H}_6/\text{C}_3\text{H}_8$ mixtures may contain small amount of other gas impurities including methane and ethane.^{44,45} The effect of these impurities on the separation performance was investigated by a breakthrough experiment of quaternary gas mixture $\text{CH}_4/\text{C}_2\text{H}_6/\text{C}_3\text{H}_6/\text{C}_3\text{H}_8$ (5/5/45/45, v/v/v/v). As expected, Co-gallate can adsorb C_3H_6 from the mixture exclusively and CH_4 , C_2H_6 , and C_3H_8 eluted in the first 2 min. The breakthrough result indicates that

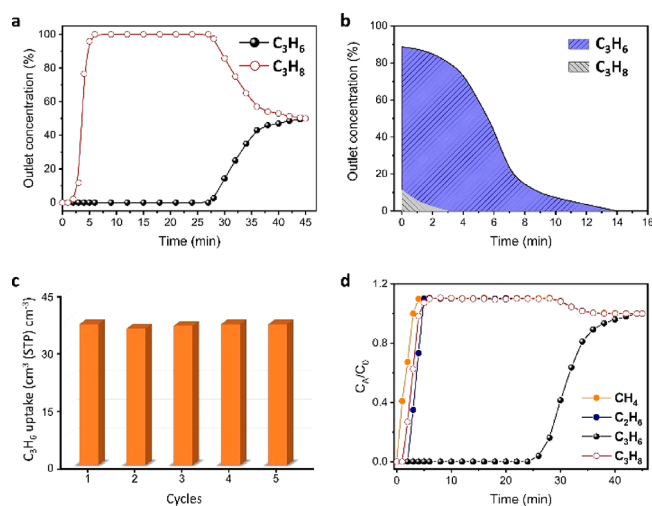


Figure 4. Column breakthrough results of Co-gallate MOF. (a) Breakthrough curves for Co-gallate MOF for an equimolar binary mixture of C_3H_6/C_3H_8 at 298 K and 1 bar. The breakthrough experiments were carried out in a packed column with 1.26 g sample at a flow rate of 1.7 mL min^{-1} . The points are experimental data, and the lines are drawn to guide the eye. (b) Concentration curve of the desorbed C_3H_6 from Co-gallate during the regeneration process. (c) Dynamic adsorption capacity of Co-gallate for C_3H_6 with five breakthrough experimental cycles. (d) Multicomponent breakthrough curves for a quaternary mixture of $CH_4/C_2H_6/C_3H_6/C_3H_8$ (5/5/45/45) at 298 K and 1 bar. The points are experimental data, and the lines are drawn to guide the eye.

Co-gallate is a very promising adsorbent for propylene recovery from multicomponent gas streams (Figure 4d and Figure S23). Considering that the material stability is very important in practical application, powder X-ray diffraction (PXRD) and gas adsorption measurements of Co-gallate were carried out after immersion in water for 7 days to examine its water stability. The PXRD result shows that the crystallinity of Co-gallate was retained upon water immersion (Figure S24). Moreover, the C_3H_6 and C_3H_8 adsorption measurements reveal that the adsorption capacity and selectivity of the water-soaked Co-gallate remain unchanged (Figures S25–29). The above results demonstrate that Co-gallate material is highly stable in water. The as-synthesized Co-gallate MOFs do not show framework decomposition until approximately $280 \text{ }^\circ\text{C}$ (Figure S30). In addition, Co-gallate can be obtained at low cost from inexpensive and readily available chemicals via a green synthetic method using only water as the solvent. Such low production cost and high sieving separation of propylene from propane endow Co-gallate with excellent potential for industrial applications.

CONCLUSIONS

In summary, by virtue of optimal pore structure and surface functionalities of MOF materials, challenging gas separations of different complexities can be realized. For the important C_3H_6/C_3H_8 separation, the above results illustrate that high sieving separation is a highly efficient approach to minimize the coadsorption of impurity components and boost the product purity. In this context, ultramicroporous MOFs featuring pore confinement and pore size matching represent potential adsorbent candidates, although there are still concerns on their separation capacity limit, material cost, and scalable synthesis. Overall, continuous research efforts on exploring

superior adsorbents for advanced adsorptive separation technologies would reap great energy benefits.

ASSOCIATED CONTENT

Supporting Information

The Supporting Information is available free of charge at <https://pubs.acs.org/doi/10.1021/jacs.0c09466>.

CIF data for Co-gallate (CIF)

CIF data for Co-gallate- C_3D_6 (CIF)

Experimental procedures, additional figures, characterizations, and additional tables (PDF)

AUTHOR INFORMATION

Corresponding Authors

Rui-Biao Lin – Department of Chemistry, University of Texas at San Antonio, San Antonio, Texas 78249-0698, United States; orcid.org/0000-0003-3267-220X; Email: ruibiao.lin@utsa.edu

Wei Zhou – NIST Center for Neutron Research, Gaithersburg, Maryland 20899-6102, United States; orcid.org/0000-0002-5461-3617; Email: wzhou@nist.gov

Banglin Chen – Department of Chemistry, University of Texas at San Antonio, San Antonio, Texas 78249-0698, United States; orcid.org/0000-0001-8707-8115; Email: banglin.chen@utsa.edu

Authors

Bin Liang – Department of Chemistry, University of Texas at San Antonio, San Antonio, Texas 78249-0698, United States

Xin Zhang – Department of Chemistry, University of Texas at San Antonio, San Antonio, Texas 78249-0698, United States; orcid.org/0000-0001-9318-8839

Yi Xie – Department of Chemistry, University of Texas at San Antonio, San Antonio, Texas 78249-0698, United States

Rajamani Krishna – Van't Hoff Institute for Molecular Sciences, University of Amsterdam, 1098, XH, Amsterdam, The Netherlands; orcid.org/0000-0002-4784-8530

Hui Cui – Department of Chemistry, University of Texas at San Antonio, San Antonio, Texas 78249-0698, United States; orcid.org/0000-0002-9723-4932

Zhiqiang Li – Department of Chemistry, University of Texas at San Antonio, San Antonio, Texas 78249-0698, United States; School of Chemical Engineering and Technology, Hebei University of Technology, Tianjin 300130, P. R. China; orcid.org/0000-0001-6901-4281

Yanshu Shi – Department of Chemistry, University of Texas at San Antonio, San Antonio, Texas 78249-0698, United States

Hui Wu – NIST Center for Neutron Research, Gaithersburg, Maryland 20899-6102, United States; orcid.org/0000-0003-0296-5204

Complete contact information is available at: <https://pubs.acs.org/doi/10.1021/jacs.0c09466>

Author Contributions

[§]B.L and X.Z contributed equally to this work.

Notes

The authors declare no competing financial interest.

ACKNOWLEDGMENTS

We acknowledge financial support from the Welch Foundation (AX-1730).

REFERENCES

- (1) Sholl, D. S.; Lively, R. P. Seven chemical separations to change the world. *Nature* **2016**, 532 (7600), 435–437.
- (2) Lin, J. Y. S. Molecular sieves for gas separation. *Science* **2016**, 353 (6295), 121–122.
- (3) Christopher, C. C. E.; Dutta, A.; Farooq, S.; Karimi, I. A. Process synthesis and optimization of propylene/propane separation using vapor recompression and self-heat recuperation. *Ind. Eng. Chem. Res.* **2017**, 56 (49), 14557–14564.
- (4) Worrell, E.; Phylipsen, D.; Einstein, D.; Martin, N., *Energy use and energy intensity of the u.s. chemical industry*. <https://www.energystar.gov>, 2000.
- (5) Li, K.; Beaver, M., *Advanced nanostructured molecular sieves for energy efficient industrial separations*. <https://www.semanticscholar.org>, 2012.
- (6) Chu, S.; Cui, Y.; Liu, N. The path towards sustainable energy. *Nat. Mater.* **2017**, 16 (1), 16–22.
- (7) Järvelin, H.; Fair, J. R. Adsorptive separation of propylene-propane mixtures. *Ind. Eng. Chem. Res.* **1993**, 32 (10), 2201–2207.
- (8) Furukawa, H.; Cordova, K. E.; O’Keeffe, M.; Yaghi, O. M. The chemistry and applications of metal-organic frameworks. *Science* **2013**, 341 (6149), 1230444.
- (9) Zhao, X.; Wang, Y.; Li, D. S.; Bu, X.; Feng, P. Metal-Organic Frameworks for Separation. *Adv. Mater.* **2018**, 30 (37), 1705189.
- (10) Li, H.; Li, L.; Lin, R.-B.; Zhou, W.; Zhang, Z.; Xiang, S.; Chen, B. Porous metal-organic frameworks for gas storage and separation: Status and challenges. *EnergyChem.* **2019**, 1 (1), 100006.
- (11) Ye, Y.; Ma, Z.; Lin, R. B.; Krishna, R.; Zhou, W.; Lin, Q.; Zhang, Z.; Xiang, S.; Chen, B. Pore Space Partition within a Metal-Organic Framework for Highly Efficient C₂H₂/CO₂ separation. *J. Am. Chem. Soc.* **2019**, 141 (9), 4130–4136.
- (12) Liang, C.-C.; Shi, Z.-L.; He, C.-T.; Tan, J.; Zhou, H.-D.; Zhou, H.-L.; Lee, Y.; Zhang, Y.-B. Engineering of pore geometry for ultrahigh capacity methane storage in mesoporous metal-organic frameworks. *J. Am. Chem. Soc.* **2017**, 139 (38), 13300–13303.
- (13) Zhou, D.-D.; Chen, P.; Wang, C.; Wang, S.-S.; Du, Y.; Yan, H.; Ye, Z.-M.; He, C.-T.; Huang, R.-K.; Mo, Z.-W.; Huang, N.-Y.; Zhang, J.-P. Intermediate-sized molecular sieving of styrene from larger and smaller analogues. *Nat. Mater.* **2019**, 18 (9), 994–998.
- (14) Hao, H.-G.; Zhao, Y.-F.; Chen, D.-M.; Yu, J.-M.; Tan, K.; Ma, S.; Chabal, Y.; Zhang, Z.-M.; Dou, J.-M.; Xiao, Z.-H.; Day, G.; Zhou, H.-C.; Lu, T.-B. Simultaneous trapping of C₂H₂ and C₂H₆ from a Ternary Mixture of C₂H₂/C₂H₄/C₂H₆ in a robust metal-organic framework for the purification of C₂H₄. *Angew. Chem., Int. Ed.* **2018**, 57 (49), 16067–16071.
- (15) Gu, C.; Hosono, N.; Zheng, J.-J.; Sato, Y.; Kusaka, S.; Sakaki, S.; Kitagawa, S. Design and control of gas diffusion process in a nanoporous soft crystal. *Science* **2019**, 363 (6425), 387–391.
- (16) Li, J.-R.; Sculley, J.; Zhou, H.-C. Metal-organic frameworks for separations. *Chem. Rev.* **2012**, 112 (2), 869–932.
- (17) Yoon, J. W.; Chang, H.; Lee, S. J.; Hwang, Y. K.; Hong, D. Y.; Lee, S. K.; Lee, J. S.; Jang, S.; Yoon, T. U.; Kwac, K.; Jung, Y.; Pillai, R. S.; Faucher, F.; Vimont, A.; Daturi, M.; Ferey, G.; Serre, C.; Maurin, G.; Bae, Y. S.; Chang, J. S. Selective nitrogen capture by porous hybrid materials containing accessible transition metal ion sites. *Nat. Mater.* **2017**, 16 (5), 526–531.
- (18) Krause, S.; Bon, V.; Senkovska, I.; Stoeck, U.; Wallacher, D.; Tobbens, D. M.; Zander, S.; Pillai, R. S.; Maurin, G.; Coudert, F. X.; Kaskel, S. A pressure-amplifying framework material with negative gas adsorption transitions. *Nature* **2016**, 532 (7599), 348–352.
- (19) Foo, M. L.; Matsuda, R.; Hijikata, Y.; Krishna, R.; Sato, H.; Horike, S.; Hori, A.; Duan, J.; Sato, Y.; Kubota, Y.; Takata, M.; Kitagawa, S. An adsorbate discriminatory gate effect in a flexible porous coordination polymer for selective adsorption of CO₂ over C₂H₂. *J. Am. Chem. Soc.* **2016**, 138 (9), 3022–30.
- (20) Lin, R.-B.; Xiang, S.; Zhou, W.; Chen, B. Microporous metal-organic framework materials for gas separation. *Chem.* **2020**, 6 (2), 337–363.
- (21) Zeng, H.; Xie, X.-J.; Xie, M.; Huang, Y.-L.; Luo, D.; Wang, T.; Zhao, Y.; Lu, W.; Li, D. Cage-interconnected metal-organic framework with tailored apertures for efficient C₂H₆/C₂H₄ separation under humid conditions. *J. Am. Chem. Soc.* **2019**, 141 (51), 20390–20396.
- (22) Cui, X.; Chen, K.; Xing, H.; Yang, Q.; Krishna, R.; Bao, Z.; Wu, H.; Zhou, W.; Dong, X.; Han, Y.; Li, B.; Ren, Q.; Zaworotko, M. J.; Chen, B. Pore chemistry and size control in hybrid porous materials for acetylene capture from ethylene. *Science* **2016**, 353 (6295), 141–144.
- (23) Chen, K.-J.; Madden, D. G.; Mukherjee, S.; Pham, T.; Forrest, K. A.; Kumar, A.; Space, B.; Kong, J.; Zhang, Q.-Y.; Zaworotko, M. J. Synergistic sorbent separation for one-step ethylene purification from a four-component mixture. *Science* **2019**, 366 (6462), 241–246.
- (24) Peng, Y.-L.; He, C.; Pham, T.; Wang, T.; Li, P.; Krishna, R.; Forrest, K. A.; Hogan, A.; Suepaul, S.; Space, B.; Fang, M.; Chen, Y.; Zaworotko, M. J.; Li, J.; Li, L.; Zhang, Z.; Cheng, P.; Chen, B. Robust microporous metal-organic frameworks for highly efficient and simultaneous removal of propyne and propadiene from propylene. *Angew. Chem., Int. Ed.* **2019**, 58 (30), 10209–10214.
- (25) Yang, L.; Cui, X.; Yang, Q.; Qian, S.; Wu, H.; Bao, Z.; Zhang, Z.; Ren, Q.; Zhou, W.; Chen, B.; Xing, H. A single-molecule propyne trap: highly efficient removal of propyne from propylene with anion-pillared ultramicroporous materials. *Adv. Mater.* **2018**, 30 (10), 1705374.
- (26) Li, L.; Lin, R.-B.; Krishna, R.; Wang, X.; Li, B.; Wu, H.; Li, J.; Zhou, W.; Chen, B. Flexible-robust metal-organic framework for efficient removal of propyne from propylene. *J. Am. Chem. Soc.* **2017**, 139 (23), 7733–7736.
- (27) Li, B.; Zhang, Y.; Krishna, R.; Yao, K.; Han, Y.; Wu, Z.; Ma, D.; Shi, Z.; Pham, T.; Space, B.; Liu, J.; Thallapally, P. K.; Liu, J.; Chrzanowski, M.; Ma, S. Introduction of π -complexation into porous aromatic framework for highly selective adsorption of ethylene over ethane. *J. Am. Chem. Soc.* **2014**, 136 (24), 8654–8660.
- (28) Bloch, E. D.; Queen, W. L.; Krishna, R.; Zadrozny, J. M.; Brown, C. M.; Long, J. R. Hydrocarbon separations in a metal-organic framework with open iron(II) coordination sites. *Science* **2012**, 335 (6076), 1606–1610.
- (29) Yang, S.; Ramirez-Cuesta, A. J.; Newby, R.; Garcia-Sakai, V.; Manuel, P.; Callear, S. K.; Campbell, S. I.; Tang, C. C.; Schroder, M. Supramolecular binding and separation of hydrocarbons within a functionalized porous metal-organic framework. *Nat. Chem.* **2015**, 7 (2), 121–129.
- (30) Bae, Y. S.; Lee, C. Y.; Kim, K. C.; Farha, O. K.; Nickias, P.; Hupp, J. T.; Nguyen, S. T.; Snurr, R. Q. High propene/propane selectivity in isostructural metal-organic frameworks with high densities of open metal sites. *Angew. Chem., Int. Ed.* **2012**, 51 (8), 1857–1860.
- (31) Li, L.; Lin, R.-B.; Krishna, R.; Li, H.; Xiang, S.; Wu, H.; Li, J.; Zhou, W.; Chen, B. Ethane/ethylene separation in a metal-organic framework with iron-peroxo sites. *Science* **2018**, 362 (6413), 443–446.
- (32) Yang, H.; Wang, Y.; Krishna, R.; Jia, X.; Wang, Y.; Hong, A. N.; Dang, C.; Castillo, H. E.; Bu, X.; Feng, P. Pore-space-partition-enabled exceptional ethane uptake and ethane-selective ethane-ethylene separation. *J. Am. Chem. Soc.* **2020**, 142 (5), 2222–2227.
- (33) Qazvini, O. T.; Babarao, R.; Shi, Z. L.; Zhang, Y. B.; Telfer, S. G. A robust ethane-trapping metal-organic framework with a high capacity for ethylene purification. *J. Am. Chem. Soc.* **2019**, 141 (12), 5014–5020.
- (34) Liao, P.-Q.; Zhang, W.-X.; Zhang, J.-P.; Chen, X.-M. Efficient purification of ethene by an ethane-trapping metal-organic framework. *Nat. Commun.* **2015**, 6, 8697.
- (35) Lin, R.-B.; Wu, H.; Li, L.; Tang, X.-L.; Li, Z.; Gao, J.; Cui, H.; Zhou, W.; Chen, B. Boosting ethane/ethylene separation within isorecticular ultramicroporous metal-organic frameworks. *J. Am. Chem. Soc.* **2018**, 140 (40), 12940–12946.
- (36) Bao, Z.; Wang, J.; Zhang, Z.; Xing, H.; Yang, Q.; Yang, Y.; Wu, H.; Krishna, R.; Zhou, W.; Chen, B.; Ren, Q. Molecular sieving of

ethane from ethylene through the molecular cross-section size differentiation in gallate-based metal-organic frameworks. *Angew. Chem., Int. Ed.* **2018**, *57* (49), 16020–16025.

(37) Cadiou, A.; Adil, K.; Bhatt, P. M.; Belmabkhout, Y.; Eddaoudi, M. A metal-organic framework-based splitter for separating propylene from propane. *Science* **2016**, *353* (6295), 137–140.

(38) Wang, H.; Dong, X.; Colombo, V.; Wang, Q.; Liu, Y.; Liu, W.; Wang, X.-L.; Huang, X.-Y.; Proserpio, D. M.; Sironi, A.; Han, Y.; Li, J. Tailor-made microporous metal-organic frameworks for the full separation of propane from propylene through selective size exclusion. *Adv. Mater.* **2018**, *30* (49), e1805088.

(39) Lin, R.-B.; Li, L.; Zhou, H. L.; Wu, H.; He, C.; Li, S.; Krishna, R.; Li, J.; Zhou, W.; Chen, B. Molecular sieving of ethylene from ethane using a rigid metal-organic framework. *Nat. Mater.* **2018**, *17* (12), 1128–1133.

(40) Geier, S. J.; Mason, J. A.; Bloch, E. D.; Queen, W. L.; Hudson, M. R.; Brown, C. M.; Long, J. R. Selective adsorption of ethylene over ethane and propylene over propane in the metal-organic frameworks M₂(dobdc) (M = Mg, Mn, Fe, Co, Ni, Zn). *Chem. Sci.* **2013**, *4* (5), 2054–2061.

(41) Bachman, J. E.; Kapelewski, M. T.; Reed, D. A.; Gonzalez, M. I.; Long, J. R. M₂(m-dobdc) (M = Mn, Fe, Co, Ni) metal-organic frameworks as highly selective, high-capacity adsorbents for olefin/paraffin separations. *J. Am. Chem. Soc.* **2017**, *139* (43), 15363–15370.

(42) Wang, Y.; Huang, N.-Y.; Zhang, X.-W.; He, H.; Huang, R.-K.; Ye, Z.-M.; Li, Y.; Zhou, D.-D.; Liao, P.-Q.; Chen, X.-M.; Zhang, J.-P. Selective aerobic oxidation of a metal-organic framework boosts thermodynamic and kinetic propylene/propane selectivity. *Angew. Chem., Int. Ed.* **2019**, *58* (23), 7692–7696.

(43) Rege, S. U.; Padin, J.; Yang, R. T. Olefin/paraffin separations by adsorption: π -complexation vs. kinetic separation. *AIChE J.* **1998**, *44* (4), 799–809.

(44) Sadrameli, S. M. Thermal/catalytic cracking of hydrocarbons for the production of olefins: A state-of-the-art review I: Thermal cracking review. *Fuel* **2015**, *140*, 102–115.

(45) Bai, S.; Sridhar, S.; Khan, A. A. Recovery of propylene from refinery off-gas using metal incorporated ethylcellulose membranes. *J. Membr. Sci.* **2000**, *174* (1), 67–79.